LOW-GRAVITY FUEL SLOSHING IN AN ARBITRARY AXISYMMETRIC RIGID TANK

by

Wen-Hwa Chu

TECHNICAL REPORT NO. 8
Contract No. NAS 8-20290
Control No. DCN 1-9-75-10050(IF)
SwRI Project No. 02-1846-02

Prepared for
George C. Marshall Space Flight Center
National Aeronautics and Space Administration
Huntsville, Alabama

SOUTHWEST RESEARCH INSTITUTE
SAN ANTONIO HOUSTON

SOUTHWEST RESEARCH INSTITUTE
Post Office Drawer 28510, 8500 Culebra Road
San Antonio, Texas 78228

LOW-GRAVITY FUEL SLOSHING IN AN ARBITRARY AXISYMMETRIC RIGID TANK

by

Wen-Hwa Chu

TECHNICAL REPORT NO. 8
Contract No. NAS 8-20290
Control No. DCN 1-9-75-10050(IF)
SwRI Project No. 02-1846-02

Prepared for
George C. Marshall Space Flight Center
National Aeronautics and Space Administration
Huntsville, Alabama

April 1969

Approved:

H. Norman Abramson

H. Norman Abramson, Director
Department of Mechanical Sciences

ABSTRACT

Solutions to free and forced oscillations have been found in terms of an auxiliary set of eigenfunctions. The slosh force and moment for an arbitrary axisymmetric rigid tank at arbitrary Bond number have been derived for both pitching and translation and expressed in terms of characteristics of an equivalent spring-mass system. Numerical examples have been constructed which compare favorably with available theories and experiments.

NOTATION

a	a reference length, say, maximum radius of the ullage
dA	$rdrd\theta$
$d\underset{\sim}{A}$	dA/a^2
dS	3-D surface element, e.g., $rd\theta drdz$
$d\underset{\sim}{S}$	dS/a^3, nondimensional surface element
F	equilibrium (mean) interface or f/a
F_e	instantaneous interface
F_H	horizontal force defined by Eq (19)
F_R	$\frac{dF}{dR}$, slope of F in the generatrix plane
F_x	x - component of force on the tank
f	equilibrium (mean) interface elevation
g	gravitational acceleration
H	amplitude of h/a, nondimensional slosh height
h	interface perturbation
h_o	a reference length, say depth of liquid at center of tank
M_o, I_o	rigid mass and moment of inertia of the mechanical model
M_F	liquid mass
M_y	pitching moment about y-axis
m_k	k^{th} slosh mass
N_B	Bond number
n	outer normal
n_o	n/a, nondimensional normal distance

p	pressure
p_I	equilibrium liquid pressure at origin - a constant
p_u	ullage pressure
p_{u_I}	equilibrium ullage pressure at origin - a constant
R	r/a, nondimensional radius
r, θ, z	tank fixed cylindrical coordinates
t	time
V	volume of the liquid divided by a^3
V_L	liquid volume (lower fluid)
W	wall wetted by liquid
W_e	instantaneous wetted wall below instantaneous interface, F_e
x_o	translational amplitude in x_s-direction
x_s, y_s, z_s	space-fixed rectangular coordinates
Γ	γa, nondimensional hysteresis coefficient
γ	hysteresis coefficient
$\Delta\rho$	density difference, $\rho - \rho_u$
δ_{ij}	Kronecker delta
ϵ_1	sign of $n \cdot \hat{z}$, $\cos(n, z)$, or $\frac{\partial z}{\partial n}$
θ_y	amplitude of pitching about y-axis
κ	the mean curvature
κ'	perturbation of the mean curvature
λ_j	j^{th} eigenvalue ($m = 1$)
λ_{mj}	j^{th} eigenvalue corresponds to m^{th} circumferential mode
ρ	lower fluid density

ρ_u	density of uilage fluid (vapor or gas)
σ	surface tension
Φ	amplitude of nondimensional velocity potential, $\phi/\omega a^2$
Φ_j	velocity potential of the auxiliary eigenfunctions
Φ_k	amplitude of nondimensional potential $\phi_k/\omega a^2$
Φ_N	see Equation (15)
Φ°	amplitude of the nondimensional potential $\phi^{\circ}/\omega^{\circ} a$
ϕ	velocity potential
ϕ_k	velocity potential of the k^{th} natural mode
ϕ'	additional velocity potential due to interface movement
ϕ°	velocity potential of liquid with a frozen interface
ω	frequency of oscillation
ω_k	k^{th} natural frequency
Ω^2	$\rho a^3\omega^2/\sigma$, product of Bond number and frequency parameter

Subscripts

$(\ )_I$	$(\ )$ at the vertex of the equilibrium interface (origin)
$(\ )_{II}$	$(\ )$ at the contact point in the generatrix plane
$(\ )_{C.G.}$	$(\ )$ related to center of gravity
$(\ )_e$	effective value of $(\ )$
$(\ )_F$	$(\ )$ on F
$(\ )_m$	$(\ )$ associated with cos $(m\theta)$ mode
$(\ )_p$	$(\ )$ related to pitching

$(\ )_T$	$(\ )$	related to translation
$(\ )_W$	$(\ )$	on W
$(\ )_u$	$(\ )$	related to the ullage
$(\ )_-$	$(\ )$	just below the interface
$(\ )_+$	$(\ )$	just above the interface

TABLE OF CONTENTS

INTRODUCTION

The behavior and consequences of fuel sloshing in rockets under a high effective gravity were recognized problems which have been quite well understood (Refs. 1, 2, and 3). The problem of low-gravity fuel sloshing, characterized by the significant role of interfacial tension, is now a subject of importance for application to coasting rockets or orbital stations.

The equilibrium behavior of fluids at zero and/or low gravity has been studied in References 4 through 7. The theoretical determination of an equilibrium interface shape is nonlinear and requires a trial and error procedure for a given contact angle (Refs. 5 and 6).

Satterlee and Reynolds (Ref. 8) have successfully solved the free sloshing problem in cylindrical containers under low gravity and formulated a variational principle for this purpose. Yeh (Ref. 9), using a similar approach, solved the free and forced sloshing problem under low-gravity conditions, without force and moment or an equivalent mechanical model. Dodge and Garza (Refs. 10 and 11) performed force measurements under simulated low-gravity conditions and predicted forces of moment for circular cylindrical tanks under lateral (translational) motion. The equivalent spring-mass model was given in Reference 10. Additional work by Dodge and Garza for other special tanks was given in References 12 and 13. A finite difference approach with application to a hemispherically bottomed cylindrical tank was given by Concus, Crane, and Satterlee in Reference 14.

These investigations indicate a need of a program for a general axisymmetric tank. A preliminary study on liquid sloshing in an arbitrary axisymmetric tank was reported in Reference 15, but it is limited to translational oscillations. It is the object of the present paper to present a semi-numerical approach for an arbitrary axisymmetric tank with simplified force and moment calculations and the resultant mechanical model for both pitching and translational oscillations. A general computer program will be completed to obtain sloshing frequencies, slosh mass, and mass-height, for which a brief description is given in the Appendix.

Governing Equations

Assuming irrotational incompressible flow, there is a space-fixed velocity potential ϕ satisfying the Laplace equation

$$\nabla^2\phi = 0 \tag{1}$$

As in thin airfoil theory, the velocity potential can be obtained by imposing boundary conditions on the initial or mean position, but the hydrostatic pressure due to gravity possesses components along both the tank axis z and the lateral axis x (Fig. 1) for pitching oscillations. The linearized Bernoulli's equation states

$$p - p_I + \rho \frac{\partial \phi}{\partial t} + \rho g (z - x\theta_y) = 0 \tag{2}$$

and

$$p - p_{u_I} + \rho_u \frac{\partial \phi_u}{\partial t} + \rho_u g (z - x\theta_y) = 0 \tag{3}$$

for the liquid and the ullage, respectively, and p_I, p_{u_I} are constants.

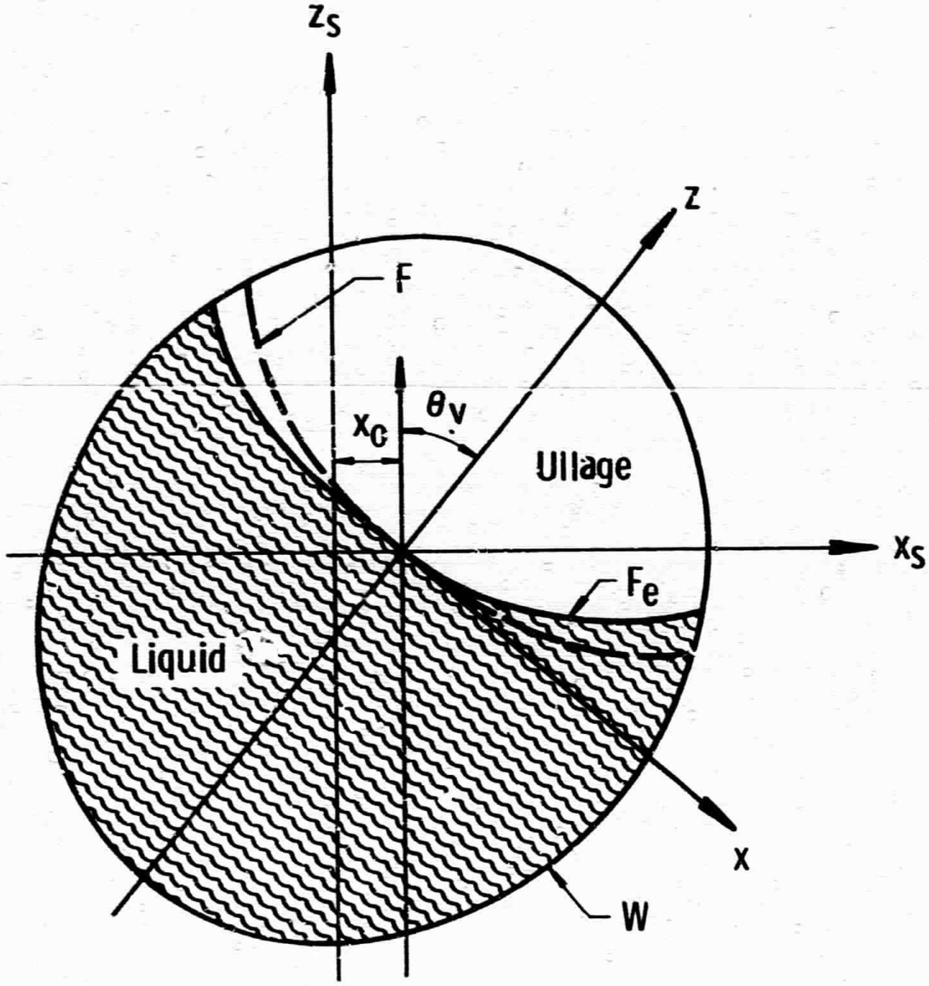

Figure 1. Some Nomenclatures

Boundary Conditions

The linearized interface kinematic condition states

$$\frac{\partial h}{\partial t} \cong \frac{\partial \phi}{\partial n} \sqrt{1 + \left(\frac{\partial f}{\partial r}\right)^2}\, \epsilon_1 \tag{4}$$

where

$$\epsilon_1 = \mathrm{sgn}\, (\underset{\sim}{n} \cdot \hat{z}) \tag{4a}$$

The interface dynamic condition states

$$p_- - p_+ = \sigma\kappa = \sigma\kappa_0 + \sigma\kappa' \tag{5}$$

For the "mean" interface location f (in general, $p_I = p_I^\circ + p_I'$, p_I°, p_I' being constants),

$$\sigma\kappa_0 + (\rho - \rho_u)\, gf - (p_I^\circ - p_{u_I}^\circ) = 0 \tag{6}$$

where the curvature of the mean interface, κ_0, is axisymmetric and

$$\kappa_0 = -\frac{1}{r}\frac{\partial}{\partial r}\left\{ \frac{r\,\dfrac{\partial f}{\partial r}}{\sqrt{1 + \left(\dfrac{\partial f}{\partial r}\right)^2}} \right\} \tag{6a}$$

Equation (6) holds for r = 0, thus

$$p_I^\circ - p_{u_I}^\circ = -2\left(\frac{\partial^2 f}{\partial r^2}\right)_I$$

The linearized interface dynamic condition is then

$$- (p'_u - p'_{u_I}) + \sigma\kappa' + \rho \frac{\partial\varphi}{\partial t} - \rho_u \frac{\partial\phi_u}{\partial t} + (\rho - \rho_u)\, gh - (\rho - \rho_u)\, gx\theta_y = 0 \qquad (7)\dagger$$

where the perturbation curvature for cos $(m\theta)$ variation

$$\kappa' = -\left\{ \frac{1}{r}\frac{\partial}{\partial r}\left[\frac{r\dfrac{\partial h}{\partial r}}{\sqrt{1+\left(\dfrac{\partial f}{\partial r}\right)^2}}\right] - \frac{m^2}{r^2}\frac{h}{\sqrt{1+\left(\dfrac{\partial f}{\partial r}\right)^2}} \right\} \qquad (7a)$$

m being unity for lateral excitation of a rigid tank. At point I, the origin, $h = 0$, $\phi = 0$, $\kappa' = 0$, and thus $p_I = p_{u_I}$. For most analyses, $\rho_u = 0$ was assumed. We shall assume the impulsive pressure in the ullage is negligible, i.e., $\phi_u \doteq 0$. Then for sinusoidal oscillations, Equations (7) and (4) yield

$$-\left\{\frac{1}{R}\frac{\partial}{\partial r}\left[R\frac{\partial H}{\partial r}\left(1 + F_R^2\right)^{-3/2}\right] - \frac{m^2 H}{R^2}\left(1 + F_R^2\right)^{-1/2}\right\} + N_{B_e} H$$
$$+ \Omega^2\Phi = 0 \text{ on F} \qquad (7b)\ddagger$$

The boundary condition on the wall is that the relative normal velocity be zero, i.e., with $\cos(n, x) = \frac{\partial x}{\partial n}$ and $\cos(n, z) = \frac{\partial z}{\partial n}$,

$$\frac{\partial\varphi}{\partial n} = \dot{x}_o \frac{\partial x}{\partial n} \qquad (8)$$

---

†For sinusoidal oscillations and $m = 1$, $h = 0$, $\phi = \phi_u = 0$, $x = 0$, and $\kappa' = 0$ at point I, thus $p'_I - p'_{u_I} = 0$. For other m values, $p'_I - p'_{u_I} = \sigma\kappa'_I$, which will be omitted until needed.

‡For sinusoidal oscillations, without loss of generality, $\dot{x}_o$, $\dot{\theta}_y$, ϕ are assumed to be proportional to sin (ωt) while h is proportional to cos (ωt).

and

$$\frac{\partial \phi}{\partial n} = \dot{\theta}_y \left(z \frac{\partial x}{\partial n} - x \frac{\partial z}{\partial n} \right) \tag{9}$$

for translational and pitching oscillations, respectively.

In addition, there is an interface contact point condition which takes the form (Refs. 8, 9 and 15)

$$\frac{\partial h}{\partial r} = \gamma h \qquad \text{at point II} \tag{10}$$

where γ may be a frequency-dependent constant. However, if the contact angle remains constant and if the not well-defined second derivative at the contact point is neglected, we can show that $\gamma = 0$ (Ref. 15). This value has been successfully used in References 10, 11, 12, and 13.

Method of Solution

We shall decompose ϕ into two parts, ϕ' and ϕ°: ϕ° is the velocity potential corresponding to a liquid contained by a rigid mean interface and the tank walls. Therefore, it satisfies the Laplace equation and the boundary condition on the contour, Equation (8) for translation and Equation (9) for pitching on F_e and W_e. It is noted that

$$\phi_T^\circ = \dot{x}_0 x \tag{11}$$

while ϕ_P° can be constructed numerically.

ϕ' is the perturbed velocity potential due to sloshing which is governed by the interface conditions and zero normal velocity condition at the wall.

We shall employ a set of auxiliary characteristic functions,* ψ_j orthogonal on the curved interface and vanishing on the walls, instead of constructing natural modes directly. The natural modes and frequencies are then calculated in terms of a truncated series satisfying the free sloshing ($\phi° = 0$, $\theta_y = 0$) inter-surface condition by the Galerkin method (Ref. 17).

The velocity potential ϕ' for forced oscillations is then calculated by expansion into normal modes and the interface condition is again satisfied by the Galerkin method.

The force and moment are obtained by integration of pressure, not only on the wall, but also on the interface since the direct surface tension force and moment on the tank is equivalent to those on the interface due to pressure, assuming the interface inertia is negligible as well as the interface mass. To put results in the mechanical model form, the divergence theorem has been most useful (with some easy manipulations).

Analytical Results

Free Oscillations

For free oscillations, the natural mode ϕ_k is expanded into a truncated series of the auxiliary eigenfunctions, i.e.,

$$\Phi_k = \frac{\phi_k}{\omega_a^2} = \sum_{j=1}^{j_{mx}} c_{k_j} \psi_{m_j} \cos(m\theta) \qquad \psi_j = \psi_{m_j} \cos(m\theta) \qquad (12a, b)$$

---

*For direct application of the Winslow method (Ref. 16), we impose the simpler normal derivation condition, $\partial\psi_j / \partial n_0 = \lambda\psi_j$, on F and used the well-known influence coefficient technique to determine the eigenvector ψ_j on the inter-surface, the eigenvalue λ_j, and ψ_j on the wall.

c_{k_j} is the k^{th} eigenvector of the following matrix equation obtained by the Galerkin method from integrating the nondimensional Equation (7b) with weighting function ψ_{m_i}

$$\left\{-\Gamma[\nu_{m_{ij}}] + [\gamma_{m_{ij}}] + m^2[\epsilon_{m_{ij}}] + \frac{\Delta\rho}{\rho} N_B [\beta_{m_{ij}}] - \Omega^2[\Delta_{m_{ij}}]\right\}$$

$$\left\{c_j\right\} = 0 \; ; \; i, j = 1 \text{ to } J_{mx} \qquad (13)$$

where

$$\beta_{m_{ij}} = \frac{\lambda_{m_j}}{a^2_{m_i}} \int_F \psi_{m_i} \psi_{m_j} dS = \lambda_{m_j} \delta_{ij} \qquad (13a)*$$

$$\epsilon_{m_{ij}} = \frac{\lambda_{m_j}}{a^2_{m_i}} \int_F \frac{\psi_{m_i} \psi_{m_j}}{R^2\sqrt{1+F^2_R}} dS \qquad (13b)$$

$$\nu_{m_{ij}} = \frac{2\pi\lambda_{m_j}}{a^2_{m_i}} [R\psi_{m_i} \psi_{m_j}] \frac{\epsilon_1}{(1 + F^2_R)_{II}} \qquad (13c)$$

$$\gamma_{m_{ij}} = \frac{\lambda_{m_j}}{a^2_{m_i}} \left\{\int_F [1+F^2_R]^{-3/2} \frac{d\psi_{m_i}}{dR} \frac{d\psi_{m_j}}{dR} dS + \int_F \frac{F_R F_{RR}}{(1+F^2_R)} \cdot \frac{d\psi_{m_i}}{dR} \psi_{m_j} dS\right\} \qquad (13d)$$

$$\Delta_{m_{ij}} + \frac{1}{a^2_{m_i}} \int_F \frac{\psi_{m_i} \psi_{m_j}}{\sqrt{1 + F^2_R}} dS \qquad (13e)$$

---

*The orthogonality property of ψ_j, thus, ψ_{m_j} can be easily proved (Ref. 15) as in the high-G case.

$$a_{m_i}^2 = \int_F \frac{\psi_{m_i}^2 \, dS}{\sqrt{1+F_R^2}} \tag{13f}$$

and m = 1 for lateral excitation of a rigid tank.

Forced Oscillations

Let

$$\phi' = -\omega^2 a \sum_{k=1}^{K_{mx}} d_k \Phi_k \quad ; \quad d_k = \frac{\bar{d}_k \Omega^2}{\Omega_k^2 - \Omega^2} \quad ; \quad \Phi_k = \sum_{j=1}^{J_{mx}} c_{k_j} \phi_j$$

(14a, b, c)

in order to satisfy the interface condition that

$$\sum_{k=1}^{K_{mx}} d_k (\Omega_k^2 - \Omega^2) \Phi_k = -\Omega^2 \Phi_0 \quad \epsilon_2 N_B \frac{\Delta\rho}{\rho} \frac{x}{a} \theta_r \equiv \Phi_N \Omega^2 \tag{15}$$

$\epsilon_2 = 0$ for translational oscillation, $\epsilon_2 = 1$ for pitching oscillation.

We have by the Galerkin procedure

$$\sum_{k=1}^{K_{mx}} \bar{d}_k \int_F \Phi_k (-H_\ell) \, d\underset{\sim}{A} = \int \Phi_N (-H_\ell) \, d\underset{\sim}{A} \quad , \quad \ell = 1 \text{ to } K_{mx} \tag{16}$$

$\bar{d}_k$ can be solved from Equation (16) by matrix inversion. There is no need of storing information of ϕ_j inside the fluid domain as only the force and moment are of interest. It is noted in the limit (Refs. 8 and 9)

$$\int_F \Phi_k (-H_\ell) \, d\underset{\sim}{A} = \delta_{k\ell} \int_F \Phi_k (-H_\ell) \, d\underset{\sim}{A} \tag{17}^*$$

*This will be referred to as biorthogonal relation.

then

$$\bar{d}_\ell = \int_F \Phi_N(-H_\ell)\, d\underset{\sim}{A} \Big/ \int_F \Phi_\ell(-H_\ell)\, d\underset{\sim}{A} \tag{18}$$

which was utilized in proving that a unique spring-mass system exists for both pitching and t: nslation.

Force and Moment

The force a.id moment exerted by a spring mass system (Fig. 2) without damping can be written in the following form (Ref. 18)

$$F_H = F_x - M_F g \theta_y \tag{19}$$

$$F_{H_T} = x_0 \omega^2 M_F \left\{ 1 + \sum_{k=1}^{\infty} \frac{m_k}{M_F} \frac{1}{\left(\frac{\omega_k^2}{\omega^2} - 1\right)} \right\} \tag{20}$$

$$M_{y_T} = x_0 \omega^2 M_F h_0 \left\{ -\frac{z_{C.G.}}{h_0} + \sum_{k=1}^{\infty} \frac{m_k}{M_F}\left(\frac{z_k}{h_0} + \frac{a}{h_0 \omega^2}\right) \frac{1}{\left(\frac{\omega_k^2}{\omega^2} - 1\right)} \right\} \tag{21}$$

$$F_{H_p} = \theta_y \omega^2 M_F h_0 \left\{ \frac{z_{C.G.}}{h_0} + \sum_{k=1}^{\infty} \frac{m_k}{M_F}\left(\frac{z_k}{h_0} + \frac{a}{h_0 \omega^2}\right) \frac{1}{\left(\frac{\omega_k^2}{\omega_2} - 1\right)} \right\} \tag{22}$$

$$M_{y_p} = \theta_y \omega^2 M_F h_0^2 \left\{ \frac{I_F}{M_F h_0^2} + \sum_{k=1}^{\infty} \frac{m_k}{M_F}\left(\frac{z_k}{h_0} + \frac{a}{\omega^2 h_0}\right)^2 \frac{1}{\left(\frac{\omega_k}{\omega^2} - 1\right)} \right\} + \theta_y g M_F h_0 \left(\frac{z_{C.G.}}{h_0}\right) \tag{23}$$

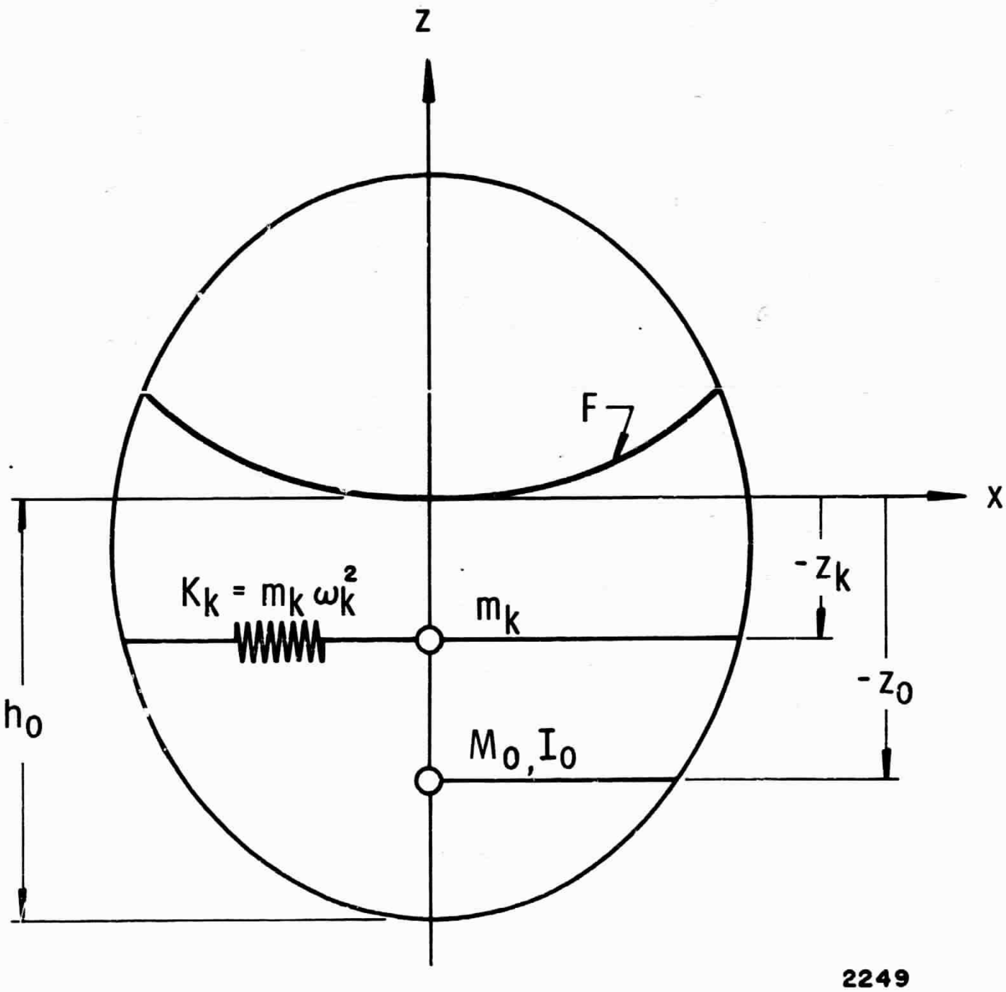

Figure 2. Equivalent Mechanical Model

with rigid mass m_0, its location z_0, and moment of inertia I_0 given by

$$\frac{m_0}{M_F} = 1 - \sum_{k=1}^{\infty} \frac{m_k}{M_F} \tag{24}$$

$$\frac{z_0}{h_0} = \frac{1}{\frac{m_0}{M_F}} \left[\frac{z_{C.G.}}{h_0} - \sum_{k=1}^{\infty} \frac{z_k}{h_0} \frac{m_k}{M_F} \right] \tag{25}$$

$$\frac{I_0}{M_F h_0^2} = \frac{I_F}{M_F h_0^2} - \left(\frac{m_0}{M_F} \frac{z_0^2}{h_0^2} + \sum_{k=1}^{\infty} \frac{m_k}{M_F} \frac{z_k^2}{h_0^2} \right) \tag{26}$$

Since the force due to liquid pressure, F_x, is

$$F_x = \int_{W_e + F_e} p \frac{\partial x}{\partial n} \, dS \tag{27}$$

and the moment due to liquid pressure M_y is

$$M_y = \int_{W_e + F_e} p \left(z \frac{\partial x}{\partial n} - x \frac{\partial z}{\partial n} \right) dS \tag{28}$$

it can be shown that

$$\frac{m_k}{M_F} = d_{k_T} f_k' \frac{1}{V} \tag{29}$$

where

$$f_k' = \sum_{j=1}^{\infty} c_{k_j} \int_F \lambda_j \psi_j \frac{x}{a} \, d\underset{\sim}{S} \tag{29a}$$

$$\bar{d}_{k_T} = \frac{1}{\beta_k^2} \int_{W+F} \Phi_k \frac{\partial x}{\partial n} d\underset{\sim}{S} \cong \frac{1}{\beta_k^2} \sum_{j=1}^{J_{mx}} c_{k_j} \lambda_j \int_F \frac{x}{a} \psi_j \, d\underset{\sim}{S} \tag{29b}†$$

$$V = V_L/\rho a^3 \quad , \quad \beta_k^2 = \int_F \Phi_k(-H_k) \, d\underset{\sim}{A} \tag{29c, d}$$

and

$$\frac{z_k}{a} = \frac{1}{\frac{m_k}{M_F}} \left(\frac{\ell'_k}{V}\right) \tag{30}$$

where

$$\ell'_k = \bar{d}_{k_T} \sum_{j=1}^{\infty} c_{k_j} \mu_j \tag{30a}$$

$$\mu_j = \int_{F+W} \psi_j \left(\frac{z}{a}\frac{\partial x}{\partial n} - \frac{x}{a}\frac{\partial z}{\partial n}\right) d\underset{\sim}{S} \tag{30b}$$

and that

$$I_F = M_F a^2 I_F^* \quad , \quad I_F^* \equiv \frac{i}{V} \int_{W+F} \Phi_p^\circ \left(\frac{z}{a}\frac{\partial r}{\partial n} - \frac{x}{a}\frac{\partial z}{\partial n}\right) d\underset{\sim}{S} \tag{31a, b}$$

In deriving the mechanical model, ρ_u has been set to zero. A simple modification can be made for small ullage density by using

$$N_{B_e} = \frac{\Delta\rho}{\rho} N_B$$

† For finite J_{mx}, it was found that $\bar{d}_{k_T}$, determined by matrix inversion of Equation (16) without using biorthogonal relation, yields results in better agreement with Dodge's theory (Ref. 12) than Equation (29b) which is correct in the limit.

the effective Bond number instead of the Bond number based on the density of the liquid, provided that the dynamic pressure due to ullage motion is negligible.

Numerical Examples

The computer program has been checked out by the following examples, using the cylindrical tank results given in Reference 12 for comparison purposes.

Flat Interface with High Bond Number

$N_B = 1000$, $\frac{h_0}{a} = 2.34$, 12×18 mesh yielded

$\frac{\omega_1^2 a}{g} = 1.85$ compared with 1.847 from exact theory (Ref. 1, p 415).

$\frac{m_1}{M_F} = 0.193$ compared with 0.194 from high-G theory (Ref. 18).

$z_1 = -0.729''$* compared with -0.724" from high-G theory (Ref. 18).

Flat Interface with Low Bond Numbers

$N_B = 10$, $\frac{h_0}{a} = 2.34$, 12×18 mesh yielded

$\frac{\omega_1^2 a}{g} = 2.15$ compared with 2.46 from exact theory.

A finer mesh is required for better agreement.

Curved Interface with Low Bond Number and Zero Contact Angle

$N_B = 100$, $\frac{h_0}{a} = 2.34$, 12×18 mesh† yielded

*Here, the origin is at the vertex of the meniscus.
†12 net points on the interface and 18 net points on the "side" wall. (See Appendix)

$\frac{\omega_1^2 a}{g} = 1.810$, $\frac{m_1}{\rho a^3} = 0.442$, $z_1 = -0.734''$ ($a = 0.68''$).

compared with theoretical values of $\frac{\omega_1^2 a}{g} = 1.777$, $\frac{m_1}{\rho a^3} = 0.438$

from Reference 12.

The experimental value of $\frac{\omega_1^2 a}{g}$ lies between 1.78 to 1.80.

With a 23 X 34 mesh, the present method yielded $\frac{\omega_1^2 a}{g} = 1.789$,

$\frac{m_1}{\rho a^3} = 0.445$, $z_1 = -0.732''$. For the 12 X 18 mesh, the CDC-6600 central process time is 2 min, while for the 23 X 34 mesh it is 21 min. Most of the computing time was expended for the generation of influence coefficients, each of which is a Neumann problem. However, the influence coefficient method may be more convenient than the inversion of a large matrix if not faster. No computer running time was reported in Reference 14, which finds natural modes by (partial) matrix inversion.

Conclusion

It seems that the present method yielded a practical way of computing the fundamental natural frequency, the first slosh mass, and its location. Higher masses and locations are usually not needed for design purposes and can be obtained by using finer meshes and longer machine time. A computer program utilizing triangular meshes and Winslow method (Ref. 16) has been successfully employed and is expected to be completed in the near future for the titled problem. However, the present logical diagram may be limited to a convex axisymmetric tank for good accuracy.

ACKNOWLEDGEMENTS

The author would like to take this opportunity to thank Mr. Donald R. Saathoff, Senior Mathematician, for writing the computer program, and Dr. Franklin T. Dodge for his helpful discussions.

The present research is supported by NASA contract NAS8-20290, George C. Marshall Space Flight Center.

REFERENCES

1. Abramson, H. N. (ed.), "The Dynamic Behavior of Liquids in Moving Containers," NASA Office of Scientific and Technical Information SP-106, Washington (1966).

2. Abramson, H. N., "Dynamic Behavior of Liquids in Moving Containers," Applied Mechanics Reviews, 16, 7, pp 501-506, July 1963.

3. Cooper, R. M., "Dynamics of Liquids in Moving Containers," ARS Journal, 30, p 725, August 1960.

4. Neu, J. T. and Good, R. J., "Equilibrium Behavior of Fluids in Containers at Zero-Gravity," AIAA Journal, 1, 4, pp 814-819, April 1963.

5. Satterlee, H. M. and Chin, J. H., "Meniscus Shape Under Reduced-Gravity Conditions," Symposium on Fluid Mechanics and Heat Transfer Under Low Gravitational Conditions, June 1965.

6. Hastings, L. J. and Rutherford, R. D., "Low Gravity Liquid-Vapor Interface Shapes in Axisymmetric Containers and a Computer Solution," NASA TM X 53790, October 1968.

7. Petrash, D. A. and Otto, E. W., "Studies of the Liquid Vapor Interface Configuration in Weightlessness," ARS Space Power System Conference, Santa Monica, California. Paper No. 2514-62 (1962).

8. Satterlee, H. M. and Reynolds, W. C., "The Dynamics of the Free Liquid Surface in Cylindrical Containers Under Strong Capillary and Weak Gravity Conditions," TR LG-2, Department of Mechanical Engineering, Stanford University, May 1, 1964.

9. Yeh, Gordon C. K., "Free and Forced Oscillations of a Liquid in an Axisymmetric Tank at Low-Gravity Environments," J. Appl. Mechanics, 34, 1, pp 23-28, March 1967.

10. Dodge, F. T. and Garza, L. R., "Experimental and Theoretical Studies of Liquid Sloshing at Simulated Low Gravities," Tech. Rept. No. 2, Contract No. NAS8-20290, Control No. DCN 1-6-75-00010, SwRI Project 02-1846, Southwest Research Institute, October 1966. See also J. Appl. Mech., 34, 3, pp 555-562, September 1967.

11. Dodge, F. T. and Garza, L. R., "Simulated Low-Gravity Sloshing in a Cylindrical Tank Including Effects of Damping and Small Liquid Depth," Proc 1968 Heat Transfer and Fluid Mechanics Institute, Stanford University Press, pp 67-69, 1968.

12. Dodge, F. T and Garza, L. R., "Simulated Low-Gravity Sloshing in Spherical Tanks and Cylindrical Tanks with Inverted Ellipsoidal Bottoms," Tech Rept No. 6, Contract NAS8-20290, Control No. DCN 1-6-75-00010, SwRI Project No. 02-1846, Southwest Research Institute, February 1968.

13. Dodge, F. T. and Garza, L. R., "Slosh Force, Natural Frequency, and Damping of Low-Gravity Sloshing in Oblated Ellipsoidal Tanks," Tech Rept No. 7, Contract No. NAS8-20290, Control No. DCN 8-75-00043(IF), SwRI Project No. 02-1846, Southwest Research Institute, February 1969.

14. Concus, P., Crane, G. E., and Satterlee, H. M., "Low Gravity Lateral Sloshing in Hemispherically Bottomed Cylindrical Tanks," Proc. 1968 Heat Transfer and Fluid Mechanics Institute, Stanford University Press, pp 80-97, 1968.

15. Chu, W. H., "Low Gravity Liquid Sloshing in an Arbitrary Axisymmetric Tank Performing Translational Oscillations," Tech Rept No. 4, Contract No. NAS8-20290, Control No. DCN 1-6-75-00010, SwRI Project No. 02-1846, Southwest Research Institute, March 1967.

16. Winslow, A. M., "Numerical Solutions of the Quasilinear Poisson Equations in a Non-uniform Triangular Mesh," Journal of Computational Physics, 1, 2, pp 149-172, November 1966.

17. Sokolnikoff, I. S., "Mathematical Theory of Elasticity," 2nd edition, McGraw-Hill Book Company, Inc., New York, (1956).

18. Abramson, H. N., Chu, W. H., and Ransleben, G. E., Jr., "Representation of Fuel Sloshing in Cylindrical Tanks by an Equivalent Mechanical Model," ARS Journal, pp 1697-1705, December 1961.

APPENDIX

BRIEF DESCRIPTION OF A COMPUTER PROGRAM

The following steps of a computer program are briefly described:

Construction of a Triangular Mesh

The triangular mesh is generated as described in Reference 16 except a simple parallelogram is used as the logical diagram (Fig. 3). For a cylindrical tank of Bond number 100, the physical diagram is shown in Figure 4. The lengths of the edge of the parallelogram can be adjusted for each individual case to yield "near" uniform triangular meshes. A continuous wall needs to be broken into two parts for the logical diagram. This only affects the local distribution of the triangular mesh and has shown to yield equally good results for a half full spherical tank at high-G as well as a cylindrical tank.

Construction of the Auxiliary Characteristic Functions

The characteristic functions ϕ satisfy

$$\nabla^2\phi = 0 \qquad \text{(A-1)}$$

$$\frac{\partial\phi}{\partial n_0} = 0 \qquad \text{on } W \qquad \text{(A-2)}$$

$$\frac{\partial\phi}{\partial n_0} = \lambda\phi \qquad \text{on } F \qquad \text{(A-3)}$$

ϕ can be solved numerically with the constructed triangular mesh by Winslow method (Ref. 16). Contact point is treated as one of the mesh points as are the other boundary points. Hence, $\frac{\partial\phi}{\partial n}$ may be discontinuous at the contact point. Zero contact angle cannot be constructed graphically but results of

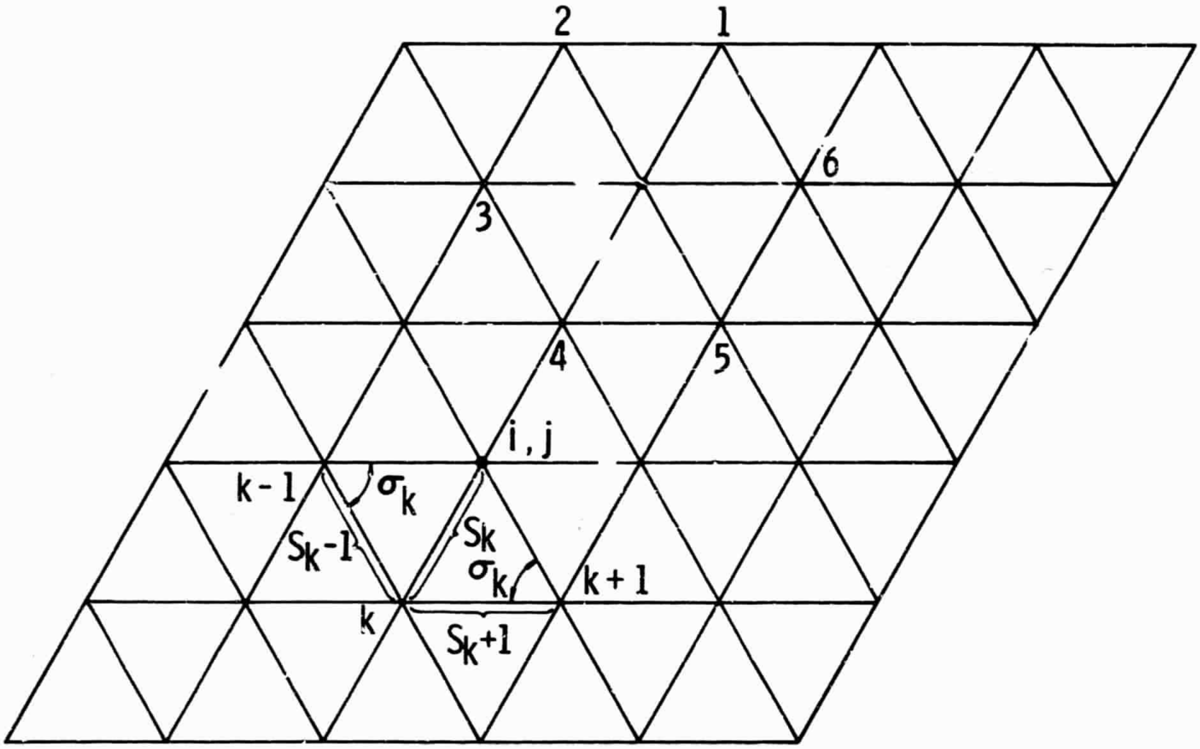

Figure 3. A Simple Logical Diagram For Triangular Mesh

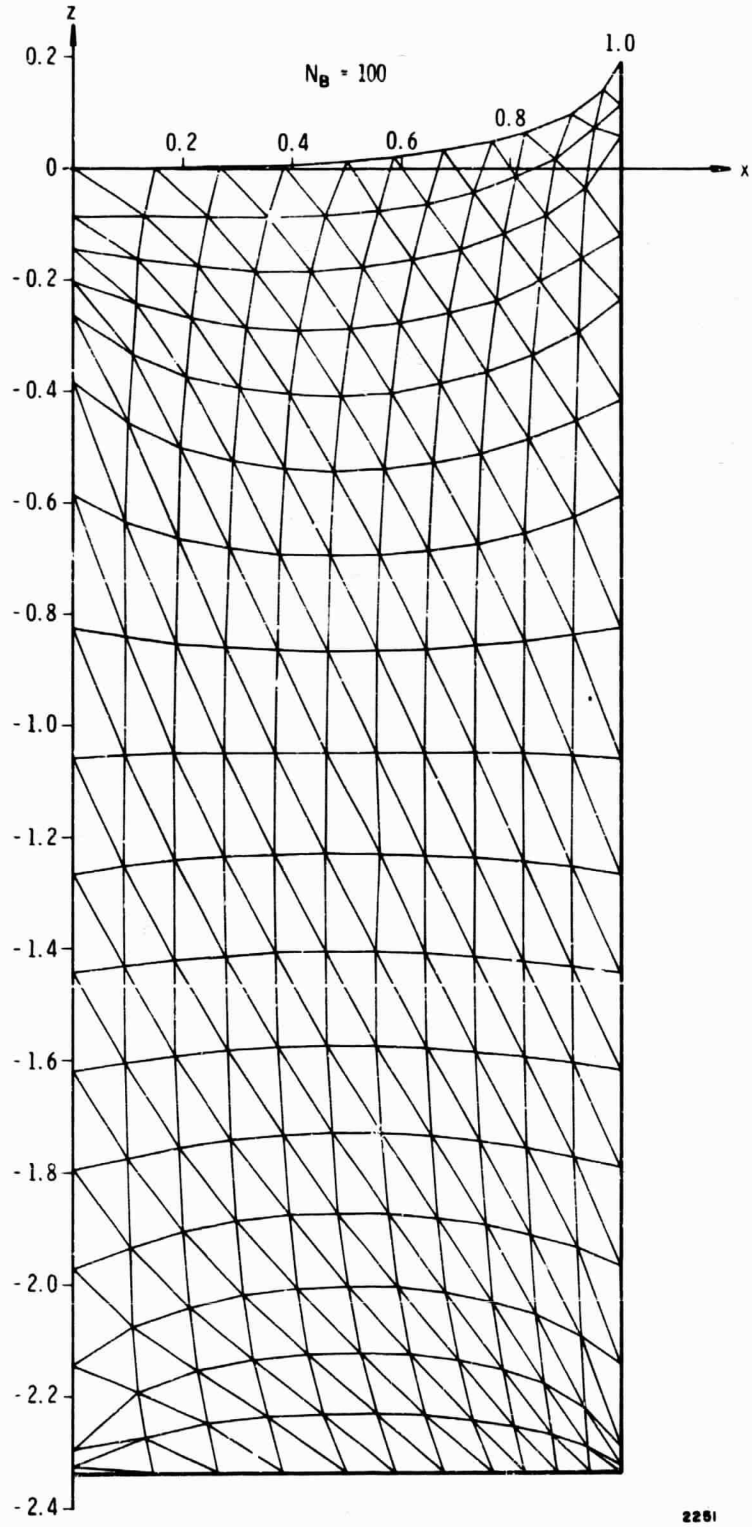

FIGURE 4. A PHYSICAL DIAGRAM OF TRIANGULAR MESH-
CYLINDRICAL TANK

decrease mesh size give closer and closer approximations to the interface and would probably lead to the correct limiting value.

For an interior joint, ij, $[\phi = \phi_{ij},\ \ \phi_k = \phi_k(i,j),\ \ r_k = r_k(i,j),\ \ r = r_{ij}]$

$$\sum_{k=1}^{6} \omega_k(\phi_k - \phi) - \frac{m^2}{r_{ij}} A_{ij}\phi = 0 \qquad \text{(A-4)}$$

where

A_{ij} is the area of the ijth dodecagon (see Ref. 16)

r_{ij} is the radius of the ijth point

$$\omega_k = \frac{1}{2}(\lambda_k \bar{r}_k \cot \theta_k + \lambda_{k-1}\ \bar{r}_{k-1} \cot \sigma_k) \qquad k = 1 \text{ to } 6 \qquad \text{(A-4a)}$$

$$\bar{r}_k = \frac{1}{3}(r_{ij} + r_k + r_{k+1}) \qquad \lambda_k = 1 \qquad \text{(A-4b, c)}$$

θ_k, σ_k (see Fig. 3) can be expressed in terms of t_k, s_{k+1}, t_{k-1}, s_{k-1}, and s_k.

For interface point,

$$\sum_{k=1}^{6} \omega_k(\phi_k - \phi) - \frac{m^2}{r_{ij}} A_{ij}\phi + \left(\frac{\partial \phi}{\partial n}\right)_{1,j} \left[\frac{1}{2} s_3 + \frac{1}{2} s_6\right] r_{ij} = 0 \qquad \text{(A-5)}$$

where

$$\lambda_6 = \lambda_1 = \lambda_2 = 0, \qquad \lambda_3 = \lambda_4 = \lambda_5 = 1$$

Note: $(\lambda_{j-1/2})$ Ref. 16 $= \lambda_{j-1}$, $(\lambda_{j+1/2})$ Ref. 16 $= \lambda_j$.

To solve for the eigenfunctions on the interface, we use influence coefficient method in which $\left(\frac{\partial \phi}{\partial n}\right)_{1,i} = 0$ except $\left(\frac{\partial \phi}{\partial n}\right)_{1,j} = 1$ for the j^{th} column of the influence matrix. A standard eigenvalue problem involving only the interface points, excluding $\phi_{1,1}$ at $r = 0$, is needed to obtain the eigenvalues λ_j and eigenvectors ψ_j. Knowing the j^{th} eigenvector on the intersurface, the corresponding value of ψ_j on the wall can be easily solved numerically again by the method of over-relaxation.

For ij^{th} point on the tank wall

$$\sum_{k=1}^{6} \omega_k(\phi_k - \phi) - \frac{m^2}{r_{ij}} A_{ij}\phi = 0 \tag{A-6}$$

$\lambda_3 = \lambda_4 = \lambda_5 = 0$ and $\lambda_1 = \lambda_2 = \lambda_6 = 1$ on the bottom wall

$\lambda_4 = \lambda_5 = \lambda_6 = 0$ and $\lambda_1 = \lambda_2 = \lambda_3 = 1$ on the side wall

On centerline, $r = 0$,

$$\begin{aligned} &\phi = 0 \text{ for } m \geq 1 \\ &\frac{\partial \phi}{\partial r} = 0 \text{ for } m = 0 \end{aligned} \tag{A-7}$$

At contact point $i = 1$, $j = j_{mx}$.

$$\sum_{k=1}^{6} \omega_k(\phi_k - \phi) - \frac{m^2}{r_{ij}} A_{ij}\phi + \left(\frac{\partial \phi}{\partial n}\right)_{1,j_{mx}} \left(\frac{1}{2} s_3\right) r_{ij} = 0 \tag{A-9}$$

$\lambda_3 = \lambda_4 = 1$, $\lambda_1 = \lambda_2 = \lambda_5 = \lambda_6 = 0$

Calculation of Natural Frequencies, Slosh Masses, and Their Location

The remaining steps are relatively routine and therefore will not be described, except it is remarked that trapezoidal rule was employed conveniently in evaluating the integrals.